minerals

MDPI

Article

Geological Controls on High-Grade Iron Ores from Kiriburu-Meghahatuburu Iron Ore Deposit, Singhbhum-Orissa Craton, Eastern India

Jitendra Prasad [1,2,*], Akella Satya Venkatesh [2], Prabodha Ranjan Sahoo [2], Sahendra Singh [2] and Nguo Sylvestre Kanouo [3]

1 Steel Authority of India Limited, Raw Materials Division, Kiriburu 833222, India
2 Department of Applied Geology, Indian Institute of Technology (Indian School of Mines), Dhanbad 826004, India; asvenkatesh@hotmail.com (A.S.V.); sahoo.prabodh@gmail.com (P.R.S.); sahendrasingh02@gmail.com (S.S.)
3 Department of Mines and Quarries, Faculty of Mines and Petroleum Industries, University of Maroua, P.O. Box 46, Maroua, Cameroon; sylvestrekanouo@yahoo.fr (N.S.K.)
* Correspondence: ism.jitendra@gmail.com

Received: 3 August 2017; Accepted: 12 October 2017; Published: 18 October 2017

Abstract: Numerous iron ore deposits are hosted within the Meso to Neo-Archean banded iron formations (BIFs) extending across the Singhbhum-Orissa Craton, eastern India. Despite the widespread distribution of BIFs, which forms part of the iron ore group (IOG), heterogeneity in their grade and mineral composition is occasionally observed even within a single ore deposit. Kiriburu-Meghahatuburu iron ore deposit (KMIOD), west Singhbhum district, Jharkhand, eastern India is characterized by a dominant hematite (often martitized) occurrence with a total resource of >150 million tonnes (MT) at 62.85 wt % Fe. Very high-grade blue dust ore (friable and powdery hematitewith~67% Fe), high-grade massive, hard laminated hematitic ores (~66% Fe) and medium to low grade goethitic/lateritic ores (50%–60% Fe) are the common iron-ore lithologies in KMIOD. These ores can be distinguished in the field from their physical appearance, meso-scale texture and spatial occurrences with the host rocks along with the variation in chemical composition. The high-grade ores are characterized by high Fe (>62 wt %), low Al_2O_3 (1.5–2.5 wt %), low SiO_2 (2.0–4.5 wt %) and low P (<0.06 wt %). Detailed field studies and laboratory investigations on the ore mineral assemblages suggest that the mineralization of high-grade iron ores at KMIOD is controlled by three major parameters, i.e., lithological, paleoclimatic and structural controls. High-grade iron ores such as blue dust seem to be formed during leaching processes through inter-bedded ferruginous shale and banded hematite jasper (BHJ) occurring within BIFs. Structural elements such as folds, joint network, fracture arrays, local faults and steeply dipping bedding planes are surmised as strong controls for the evolution of different iron ore types from the BHJ. Most of the high-grade ores are concentrated at the hinge portions of second generation folds (F_2) owing to the easy access for circulation of meteoric solution along the fractures developed due to release of stresses at the hinge portions aided by supergene ore enrichment processes. The BHJ and interbedded ferruginous shale seem to have been given a significant contribution for the formation of different grades of iron ores over the area. Lithologically, the BIFs are governed by rheological features providing channel ways in the ore enrichment process. The variation in the iron ore mineralogy is caused by the variation in depositional and paleoclimatic environment, structural setting and lithological attributes. Hence, these parameters could be used for future exploration and grade recovery of iron ore resources in the region and in the adjoining areas.

Keywords: BIFs; KMIOD; high-grade ores; BHJ; supergene ore enrichment processes

1. Introduction

The Singhbhum-Orissa Iron Ore Craton (SOIOC), eastern India, hosts one of the world's major iron ore resources. A number of high-grade (>62 wt % Fe) iron ore deposits are situated in eastern India, such as Chiria, Gua, Noamundi, Kiriburu-Meghahatuburu, Barbil, Gorumahisani, Tomka and Daitari (Figure 1). About 36% (170 MT) of the India's iron ore production comes from eastern India. Views regarding genesis, structural set up and depositional mechanism of these deposits have been proposed by several workers [1–7]. Some workers have argued in favor of a sedimentary chemogenic origin for the banded iron formations (BIFs) while a volcanogenic input for the source of iron is suggested, based on the geochemistry [8,9]. Extensive works have been carried out to understand the structural evolution and genesis of iron ore in regional scale [5–14]. In contrast, limited scientific studies have been conducted on geological controls of the banded hematite jasper (BHJ) hosted high-grade iron ore deposits at the Kiriburu-Meghahatuburu iron ore deposit (KMIOD) despite being the store house and major source of high-grade iron ore raw materials for different steel plants of India.

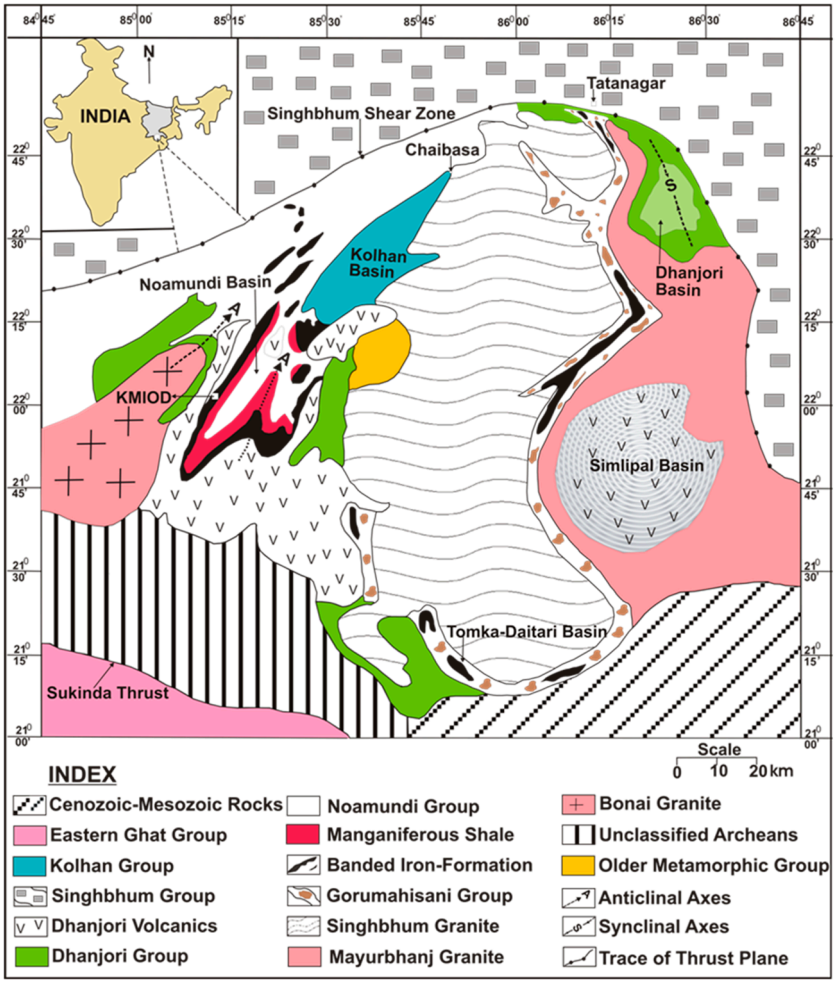

Figure 1. Geological map of Singhbhum-Orissa iron ore craton showing distribution of different lithological units. The study area Kiriburu-Meghahatuburu iron ore deposit (KMIOD) forms part of western limb of horse-shoe synclinorium modified after [10,11].

Globally, the BIFs have long been studied because they provide important clues for the understanding of oceanic water chemistry, atmospheric evolution, Proterozoic environment and the emergence of life on the Earth [15–19]. The iron ore resources at KMIOD are being developed through opencast mining operations (maximum depth of 110 m) by Steel Authority of India Limited (SAIL), a

public sector undertaking, Government of India since 1964. The KMIOD mainly supplies iron ore to its various captive steel plants of SAIL. It accounts for a total iron ore resource (proved, probable and inferred) of more than 150 MT Fe with an average grade of 62.85 ± 1.31 wt % Fe along with SiO_2 and Al_2O_3 in variable proportions (Table 1). In this study, we mainly investigate the dominant role of geological factors which are responsible for the evolution of high-grade iron ores based on field, petrographic and geochemical investigations, which could be used as potential tools for optimizing future exploration, production, reserve estimation and recovery of the iron ores at KMIOD and elsewhere in the adjoining areas.

Table 1. Resources of High-grade Iron Ores at Kiriburu-Meghahatuburu iron ore deposit (KMIOD) comprising of Meghahatuburu Iron Ore Mine (MIOM); Kiriburu Iron Ore Mine (KIOM); Central Block (CB); South Block (SB); Source: Mining Plan Division, Steel Authority of India Limited, KMIOD.

Deposits	Status	(Proved + Probable)		Inferred	
		Quantity (MT)	% Fe	Quantity (MT)	% Fe
MIOM *	Working Mine	6.50	62.80	22.85	62.51
MIOM-CB	Prospect	14.66	63.19	0.73	65.80
KIOM *	Working Mine	6.70	63.04	59.73	62.31
KIOM-SB	Prospect	32.56	62.37	7.28	66.03
Total/Average		44.74	62.85	106.17	64.16

* Resource estimate compiled as per United Nations Framework Classification (UNFC).

2. Regional Geology

The geological framework of the Meso to Neo-Archean (~3.3 Ga) iron ore deposits of Singhbhum-Orissa region was established by different workers from time to time [5,6,20,21]. The SOIOC is the oldest Archean nucleus of eastern India, a major part of which is occupied by Singhbhum granitic batholithic complex. The boundary between the Singhbhum supracrustals and SOIOC is demarcated by a prominent shear zone known as the Singhbhum shear zone (SSZ)(Figure 1). The study area is a part of the volcano-sedimentary Archean iron ore group (IOG) that hosts one of the largest Fe (+Mn) deposits of India [6,14]. The mafic volcanic rocks of the Dalma lava are younger than the IOG [21]. Several phases of Mesoarchean granitic units, namely, Singhbhum Granite and Bonai Granite, occur within the craton (Figure 1).

A major revised stratigraphic succession shows two distinct provinces in the region [22], the younger IOG to the north and the older IOG to the south, the SSZ making the boundary between the two iron ore sequences (Figure 1). In the SOIOC, an oval shaped nucleus of Archean rocks is enclosed by the Proterozoic rocks both to the north and to the south [4,23]. The SSZ marks the northern boundary of the Archean nucleus, while Sukinda thrust forms the southernmost boundary of SOIOC (Figure 1). The elongated Singhbhum Granite batholithic complexes occupy major part of the SOIOC covering about 10.000 km^2. The IOG rocks of eastern India occur in three basins which are peripheral to the Singhbhum Granite massif. The major iron ore basins of eastern India (Figure 1) in order of age, from oldest to youngest, are: Gorumahisani-Badampahar (eastern IOG), Tomka-Daitari (southern IOG) and Bonai-Keonjhar (western IOG) iron ore basins [24]. The study area is a part of the Bonai-Keonjhar Iron Ore Basin (BKIOB).

Geologically, the eastern Indian iron formations are hosted by BHJ and banded hematite quartzite (BHQ). Shallow water environment of deposition, proximal to the shoreline with a steeper paleoslope of the shelf has been considered for the BHJ formation as evidenced by the presence of numerous primary sedimentary features within it [3]. The iron ores from the BIFs have been formed due to enrichment of BHJ and ferruginous shale by gradual removal of silica under continuous leaching process [9,13]. The enrichment of BIFs was mainly facilitated by a complex interaction of BIFs with carbonic-rich and low salinity aqueous fluids of metamorphic origin and high salinity fluids of hydrothermal-magmatic

origin [25–27]. The variation in the iron ore mineralogy is caused by the variation in depositional environment; structural setting and lithological attributes. The various episodes of tectonic setting within the depositional basin resulted in the formation of low grade metamorphic sediments including tuffaceous shales, BHJ-hosted iron ores and mafic volcanic rocks.

However, there is no uniformity in the opinions among researchers of Singhbhum-Orissa geology regarding depositional environment and tectonic setting of these BIFs and several diverse opinions were proposed in this regard [4–14]. The BIFs of SOIOC, eastern India are designated as Superior type BIFs [8] in view of their association with dolomite, quartzite, shale, volcanic tuff and other volcanic rocks, while other workers termed them as Algoma type [6,7] (Figure 2). The IOG rocks have been folded into a major NNE plunging horseshoe-shaped synclinorium, overturned towards the east, and cross folded along an E–W axis [24,28]. The iron ore mineralization is mainly associated with an anticlinal structure followed by three phases (D_1, D_2 and D_3) of successive deformations [28].

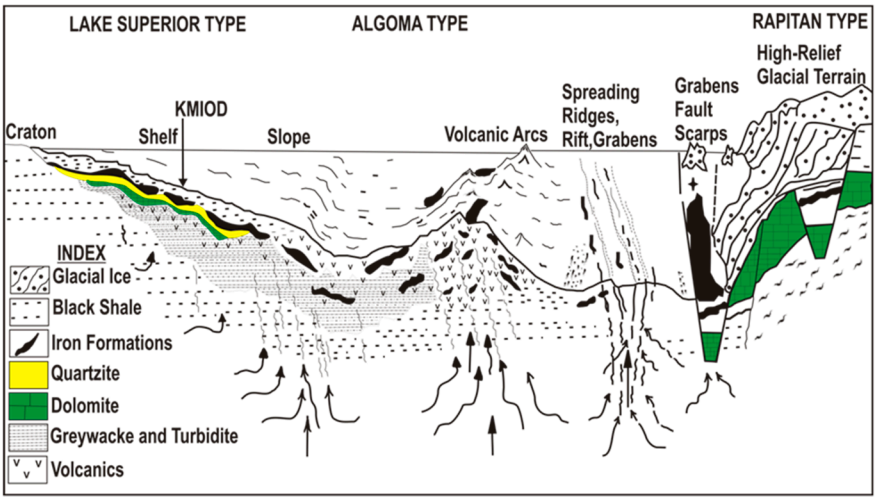

Figure 2. Distinguishing features of Lake Superior, Algoma and Rapitan types of iron formations, showing the possible position of the study area iron ore deposit (KMIOD) modified after [8,29].

3. Geology of Kiriburu-Meghahatuburu Iron Ore Deposit

The iron ore deposits of the Kiriburu-Meghahatuburu area, being a part of BKIOB, occur along the western limb of the horseshoe-shaped synclinorium (Figure 1). The BKIOB is located on the western flank of Singhbhum Granite batholithic complex in west Singhbhum-Keonjhar district, extending over a strike length of 60–70 km in NNE–SSW direction from Chakradharpur to Malangtoli. The iron ore bearing sequences of this basin overlies Older Metamorphic Group and Dhanjori Group in the east and Bonai Granite in the west and is intruded by gabbro/dolerites such as the Dhanjori lava (Figure 1). The region is folded into a north-plunging asymmetrical horseshoe-shaped synclinorium consisting of two limbs, i.e., the western limb and the eastern limb on a regional scale. The iron ore deposits along the western limb are contiguous, while those along the eastern limb are sporadic in nature (Figure 1).

The major lithological units associated with BIFs in the area are laterite, BHJ, shale (tuffaceous and ferruginous), mafic volcanics and locally formed quartzite-conglomerate sequence (Figures 3 and 4A–D). The BIFs in the area trend NE–SW to NNE–SSW direction and extends for ~7–8 km with ~4–5 km width with thickness varies from 100–120 m. The BHJ-hosted iron ores of the area comprise different varieties of iron ore types such as lateritic-limonitic ores (LAT), goethitic ores (GO), hard laminated ores (HLO), soft laminated ores (SLO) and blue dust (BD) (Figure 5A,B). The blue dust is a deep blue colored, fine powdery, hematitic iron ore containing more than 64% Fe and is considered the best grade of iron ore. Mainly, the iron ores at KMIOD are powdery (blue dust/soft friable ores) in nature, along with hard massive or laminated ores and the ratio between powdery to hard massive ore is 70:30.

The quality of the iron orevaries from place to place depending on various geological constraints, such as the degree of leaching processes, favorable lithological and structural features, tectonic setting and paleoclimatic conditions.

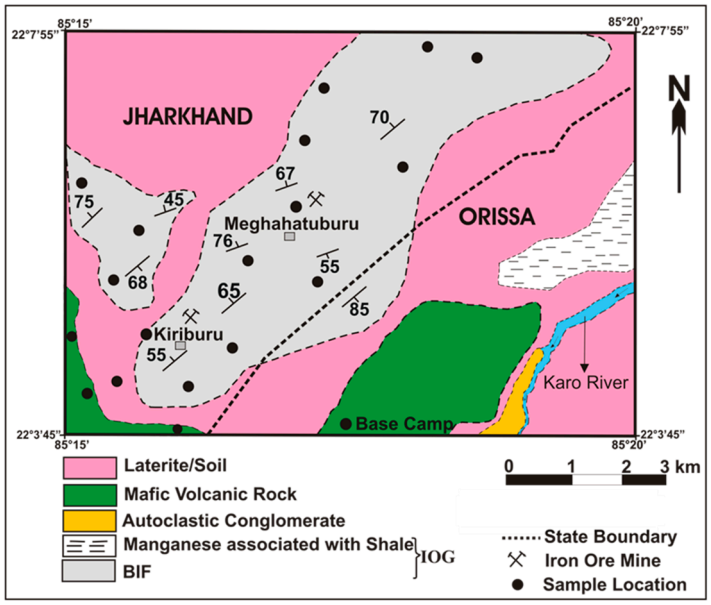

Figure 3. Deposit scale geological map of Kiriburu-Meghahatuburu mining area.

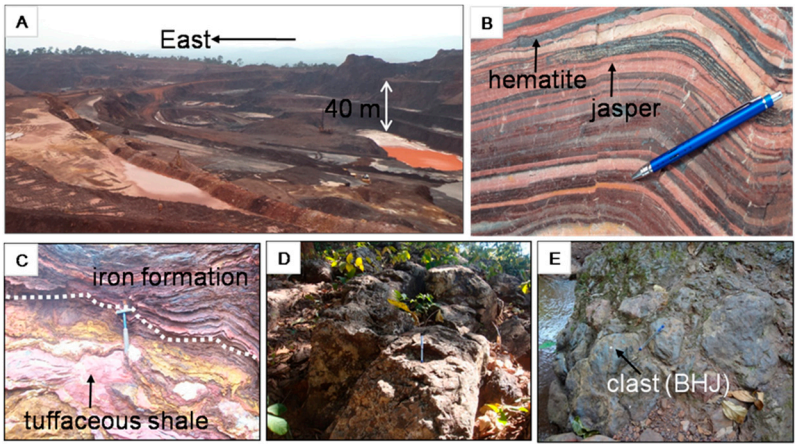

Figure 4. (**A**) Panoramic view of an open pit mining pit at KMIOD; (**B**) close-up view of deformed Banded Hematite Jasper (BHJ) with microfaults and fractures; (**C**) field photograph showing contact zone of tuffaceous shale and thin laminated BHJ; (**D**) mafic volcanic rock; and (**E**) auto-clastic conglomerate exposed along the Karo River.

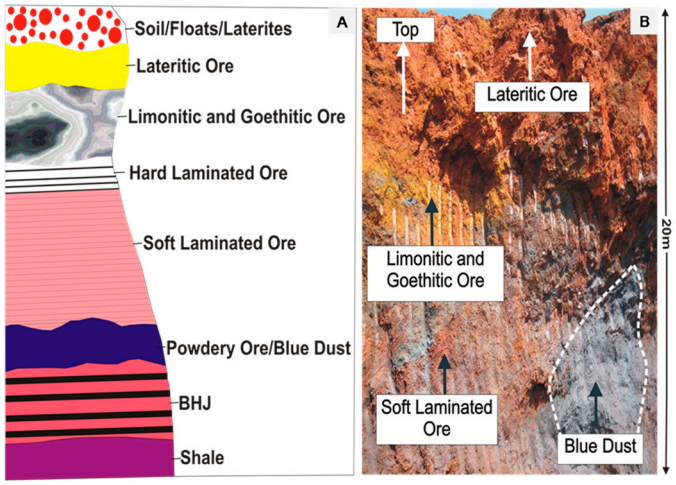

Figure 5. (**A**) Schematic diagram showing geological succession of iron ores at KMIOD; and (**B**) atypical sequence of iron ore succession from top to bottom of the iron formation seen at a mine bench (908 m of elevation) of the Kiriburu mining area.

4. Methodology

Surface lithological and structural mapping were conducted in and around open cast mining areas of Kiriburu-Meghahatuburu followed by an in-depth geological study of the iron formation. Representative samples of BHJ, iron ores and associated host rocks were collected from fresh outcrops. Sample locations are given in Figure 3. The samples of associated host rocks and iron ores were collected through channel cut and random sampling methods from the fresh exposures in and around the mining areas and from different mine benches to carry out mineralogical characterization in order to understand textural and micro-structural features. The nature of occurrences and physical properties of various types of lithological units and iron ores were studied throughout the field area. Borehole lithologs were prepared to identify the variation in depth of different types of iron ores. The orientation of bedding data was carefully measured in the field and analyzed using stereographic projection and Rose diagrams to understand the structural geometry of the area.

The samples were pulverized and subjected to qualitative XRD analysis at National Metallurgical Laboratory, Jamshedpur, India using SIEMENS D500 (Bruker, Billerica, MA, USA) having automatic divergence slit, receiving slit and graphite mono-chrometor assembly. Cu Kα radiation, operating at 40 kV and 20 nA was used and for recording the 2θ scan range from 10°–90° with a counting time of 1 s per step. Major element chemistry was undertaken using XRF spectrometry (X-ray spectrometer AXS-SRS-3400, Bruker, Billerica, MA, USA) at National Geophysical Research Institute, Hyderabad, India. During XRF analysis, Penta-erythritol (Al and Si), Thallium acid Pthalate (Na and Mg), Germanium and Lithium Fluoride analyzing crystals in vacuum medium were used for Scandium and Rhodium targets. Loss on ignition (LOI) of different ore types were estimated at Indian Institute of Technology (Indian School of Mines) Dhanbad, India.

5. Lithological Characteristics at KMIOD

The important litho units associated with BIFs in the area in order of their abundance is discussed as below.

5.1. Laterite

It represents an important lithological unit present over the area (Figures 3–5). It mainly occurs as thick capping at the top of the deposits, showing different colors varying from yellowish red to brick red. They have been formed due to a continuous leaching process under tropical climatic conditions

with high annual rainfall. At some places, they are associated with a box-work structure that develops due to leaching and indicates an underlying iron ore deposit and its associated ores below the surface.

5.2. BHJ

It is the most important and wide spread lithological unit present in the area. The iron ore resources in the area are mainly hosted with BHJ. It consists of alternate bands of hematite and jasper (Figure 4B). Different types of iron lithosomes such as evenly-banded, unevenly-banded and maculose banding have been observed within BHJ under variable energy conditions that prevailed in the depositional iron ore basin or BKIOB (Figures 4B and 6A,B). The thickness of jasper meso-bands generally ranges 2–40 mm, while that of iron-rich meso-bands ranges 1–30 mm.

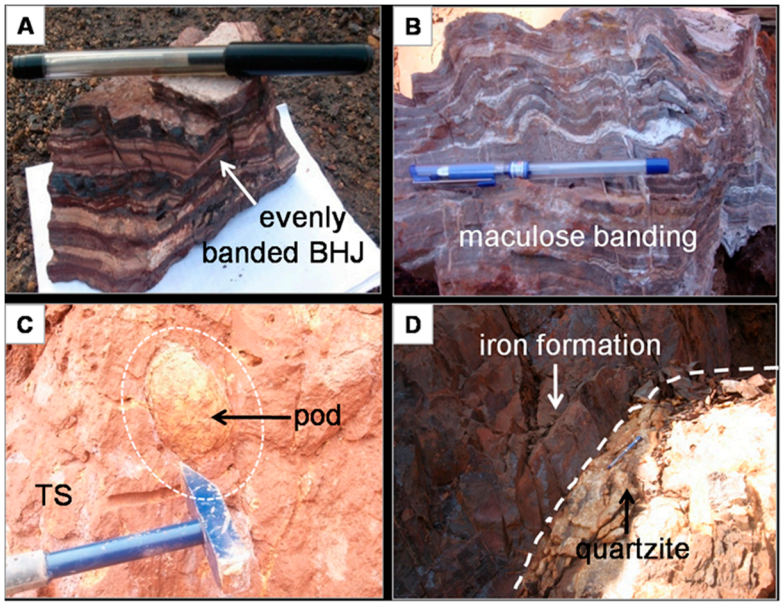

Figure 6. (**A**) Close-up view of evenly banded BHJ at places crumpled due to effect of deformation; (**B**) maculosebanding in BHJ; (**C**) pod structure occurring within tuffaceous shale (TS); and (**D**) Cherty quartzite associated with the iron formation.

5.3. Shale

Iron formation of the area is closely associated with shale. Mainly two types of shales are observed in the area, i.e., tuffaceous shale and ferruginous shale. The tuffaceous shale is originated from volcanic sources representing upper shale horizon within the iron sequences. They are massive in form and soft in nature, exhibiting different colors such as white, yellow, purple, olive brown and pinkish red (Figure 4C). At places, pod structure is also observed, which might have been formed from weathering processes, followed by secondary deposition of in-situ materials (Figure 6C,D). The tuffaceous shale is highly enriched in Si (up to 50%) and Al (up to 40%) and, thus, their association with the iron ores is one of the major factors affecting iron ore quality. The ferruginous shale, on the other hand, represents middle or lower shale that mainly occurs as inter-bedded units running parallel to the BIFs sequences. They exhibit extensive leaching process resulting into the formation of high-grade iron ores, such as blue dust in the area.

5.4. Cherty Quartzite

It is also an important rock type next to the shale formation and occurs in close association with the iron formation as a massive body or as inter-bedded unit (Figure 6E). Cherty quartzite is seen at various mine benches, which is highly fractured in nature, indicating imprint of complex deformation

in the study area. Its highly fractured nature might have provided avenue for meteoric solutions required for leaching processes during the evolution of high-grade iron ores in the area.

6. Structural Geometry and Microstructures Associated with KMIOD

Antiformal and synformal features are common within BIFs of the area which have later been modified into various classes of folds under successive deformation with varying amplitude and wavelengths (few centimeters to several meters) (Figure 7A). Secondary folds of mainly M and W patterns are also associated with various deformational phases (Figure 7B). Folds having different attitudes of fold axes are most commonly observed in the area with varying plunge (10°–45°) of fold axis which are gently to moderately plunging in nature (Figure 7C). Considerable variation in plunge and direction of the fold axis are observed in the area due to the presence of non-cylindrical folds. Reclined folds observed in the area have been formed during the third phase of deformation which might have changed the fold axis of early formed first or second generation folds from sub-horizontal to steeply plunging (Figure 7D). Kink bands (Figure 7E) are also very common in the area.

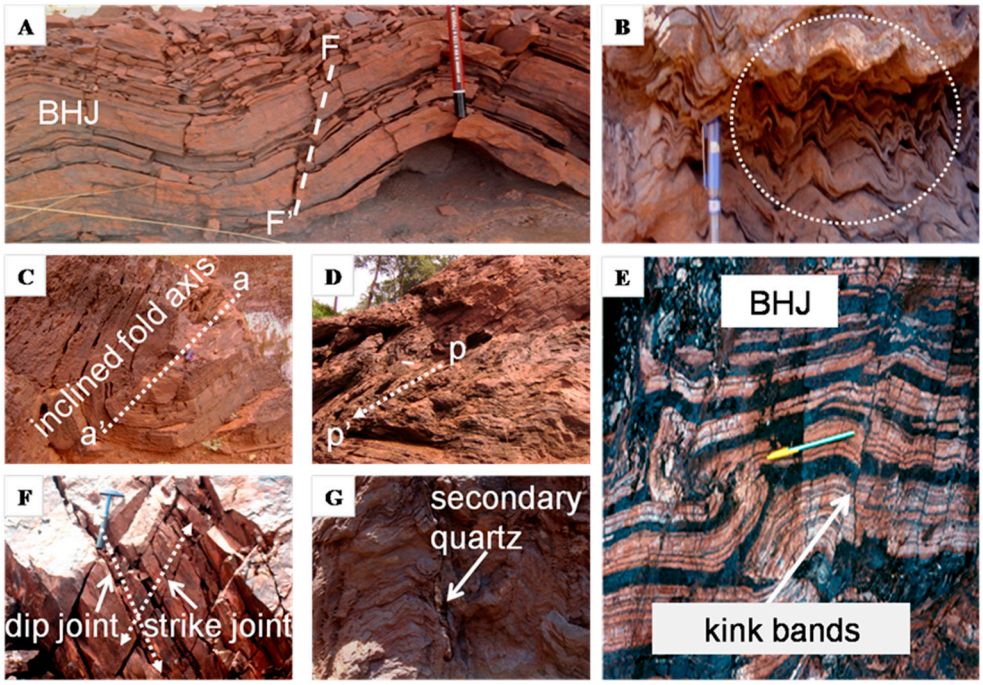

Figure 7. (**A**) Antiformal and synformal features in BHJ. Minor dislocation of bedding can be seen along FF′; (**B**) secondary folds of M-W pattern; (**C**) inclined or plunging folds in BHJ with its fold axis dipping at low angle towards NE direction; (**D**) areclined fold geometry; (**E**) kink bands in BHJ associated with younger generation folds playing significant role in ore enrichment processes through leaching; (**F**) aset of strike and dip joints developed in BHJ due to deformation; and (**G**) fractures of different orientations and dimensions in the iron formations that contain secondary minerals such as quartz, which aided the supergene process.

The iron formation exhibits the presence of three sets of joints. However, it seems that only two sets of joints (strike and dip joints) are prominent and well delineated while the third set (oblique joint) is rather sporadic in occurrence (Figure 7F). Strike joints (dip = 55°–70°) towards W–NW direction) are more dominant than dip joints. The orientation of dip joints is roughly NW–SE dipping from 65° to 85° towards SW direction. Sometimes, a set of strike and dip joints intersects to divide the iron lithosomes into equal blocks, aiding the process of supergene enrichment for the formation of different types of iron ores (Figure 7F). Large scale faults have not been observed in the iron formation of the area. However, a few minor faults sometimes filled up with secondary minerals, such as quartz have been

observed (Figure 7A). The orientation of these faults is roughly E–W dipping steeply (60°–80°) towards north. Fractures of random orientations are well observed within the iron formations at KMIOD affected by several deformational phases. Sometimes, these fractures are filled up with secondary minerals such as quartz (Figure 7G). Presence of joint sets and fractures within the iron formation provide excellent avenues for meteoric solutions to percolate downward, causing leaching of mobile components and formation of soft friable iron ore/blue dust by the enrichment process.

The area has undergone three major phases of successive deformations [5,24,28], namely D_1, D_2 and D_3, giving rise to F_1, F_2 and F_3folds, respectively, and the same has also been observed during the present field studies. The early folds are subjected to refolding, resulting in different superposition patterns. F_1 folds are generally isoclinal folds with their fold axis dipping at an angle of about 45° towards E–W to ENE–WSW. D_2 deformation resulted in the development of F_2 open to tight folds, with a fold axis trending between NE–SW and N–S, which is near co-axial to non-coaxial with F_1 folds. This near co-axial superposition of D_2 folds over D_1 resulted in the formation of hook shaped geometry or Type-III interference patterns [30]. F_3 folds nearly co-axial with F_2folds and have been developed during D_3deformation forming kink bands, which are younger than F_1 and F_2 folds. In this area, type-I and type-III superposition patterns are more common (Figure 8A). The field and structural data during the present study demonstrate that the overall structural pattern of KMIOD is anticlinal in nature based on their bedding data, which is shown in Figure 8B–D. The structural map of KMIOD is shown in Figure 9.

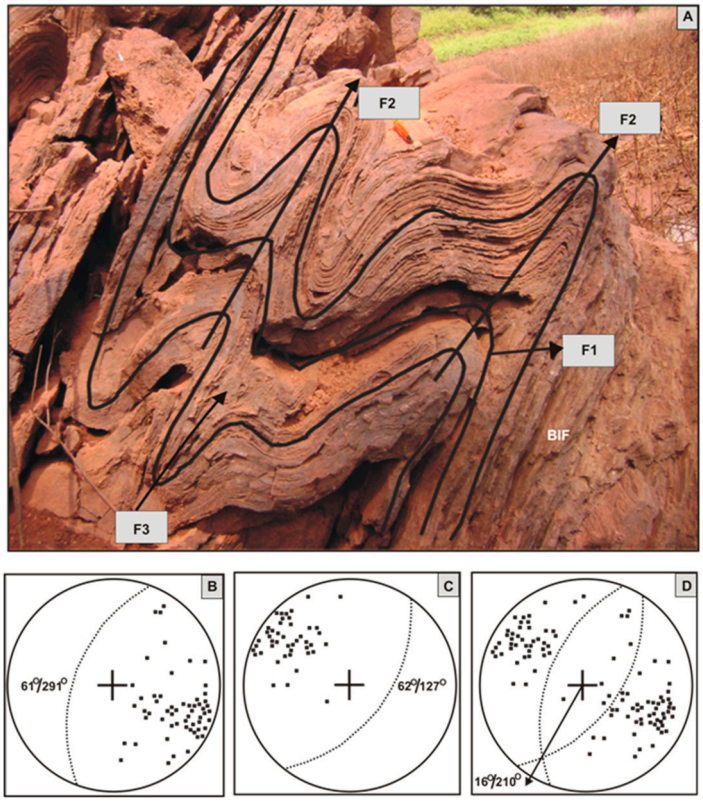

Figure 8. (**A**) Superposed pattern of folds (F_1, F_2 and F_3) developed in BHJ; (**B**) equal angle projection of the poles of the bedding data which are dipping towards west; (**C**) poles of bedding data dipping towards east; and (**D**) equal-angle projection of the poles of the bedding. The arrow mark shows the overall plunge (towards south) of the iron formation. The maximum cluster of data points of bedding are towards the eastern and western side, which indicates that the overall structural geometry of KMIOD is antiformal in nature because the dip of the beds is away from each other.

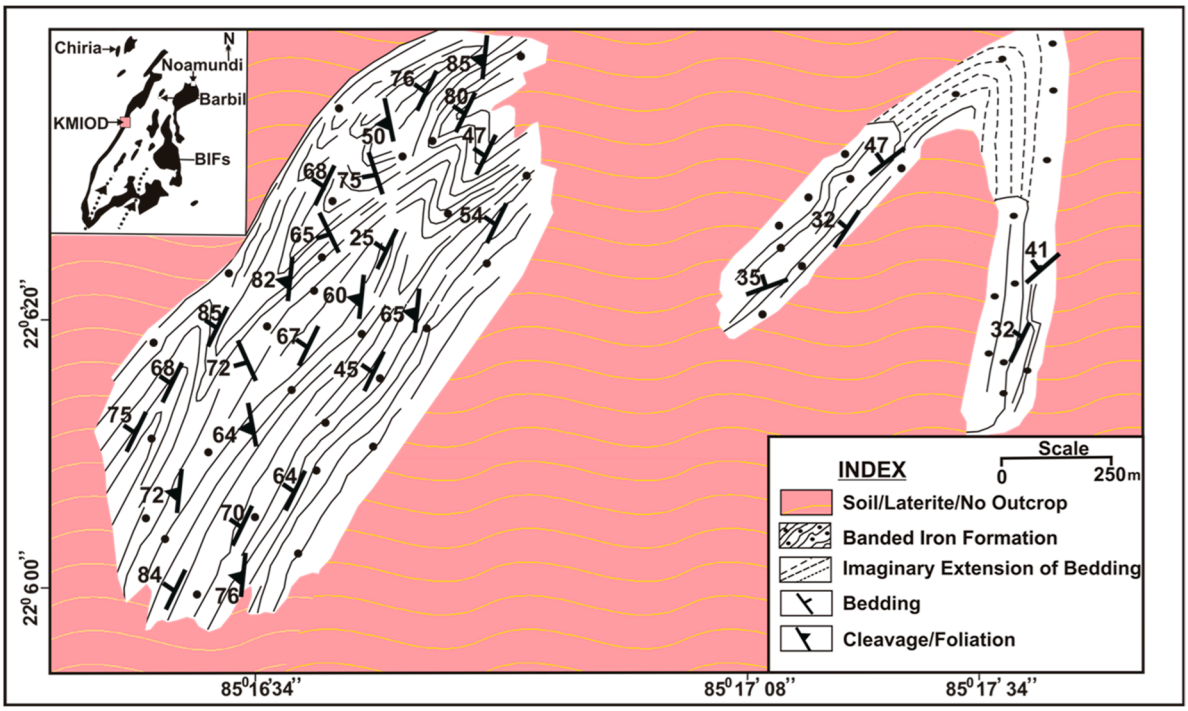

Figure 9. Structural map in and around KMIOD which forms a part of the western limb of the horse shoe-shaped synclinorium within Bonai-Keonjhar iron ore basin.

7. Iron Ore Types at KMIOD and their Mineralogical Assemblages

Field studies and ore microscopic observations envisage various types of iron ores at KMIOD with a wide range of mineralogical assemblages, which are discussed below.

7.1. Hard Massive Ore

Ore microscopy studies reveal that the mineralogy of hard massive ore (HMO) consists mainly of hematite and goethite (hematite is often martitized and the resultant product is martite which is a pseudomorph of hematite, in which magnetite is altered to hematite due to oxidation) followed by gangue minerals such as quartz (Figure 10A). The euhedral magnetite crystal shows re-crystallization process leading to the formation of hematite along the boundary and shown in Figure 10A. The HMO exhibits massive and incipient laminated structures in which micro-platy hematite (Fe_2O_3) grains form a dense network.

7.2. Hard Laminated Ore

Hard laminated ores (HLO) consist of laminated, high porosity micro-platy hematite along with some quartz in the voids and fractures (Figure 10B). The ores are steel grey in color and are relatively high-grade. They consist of both massive hematite and specular hematite bands. The presence of micro-fractures in alternating bands and silica grains in the interstitial spaces confirm that they are derived from the host BHJ (Figure 10B). During the formation of hard laminated ore, alternating bands of jasper in BHJ were replaced by secondary hematite.

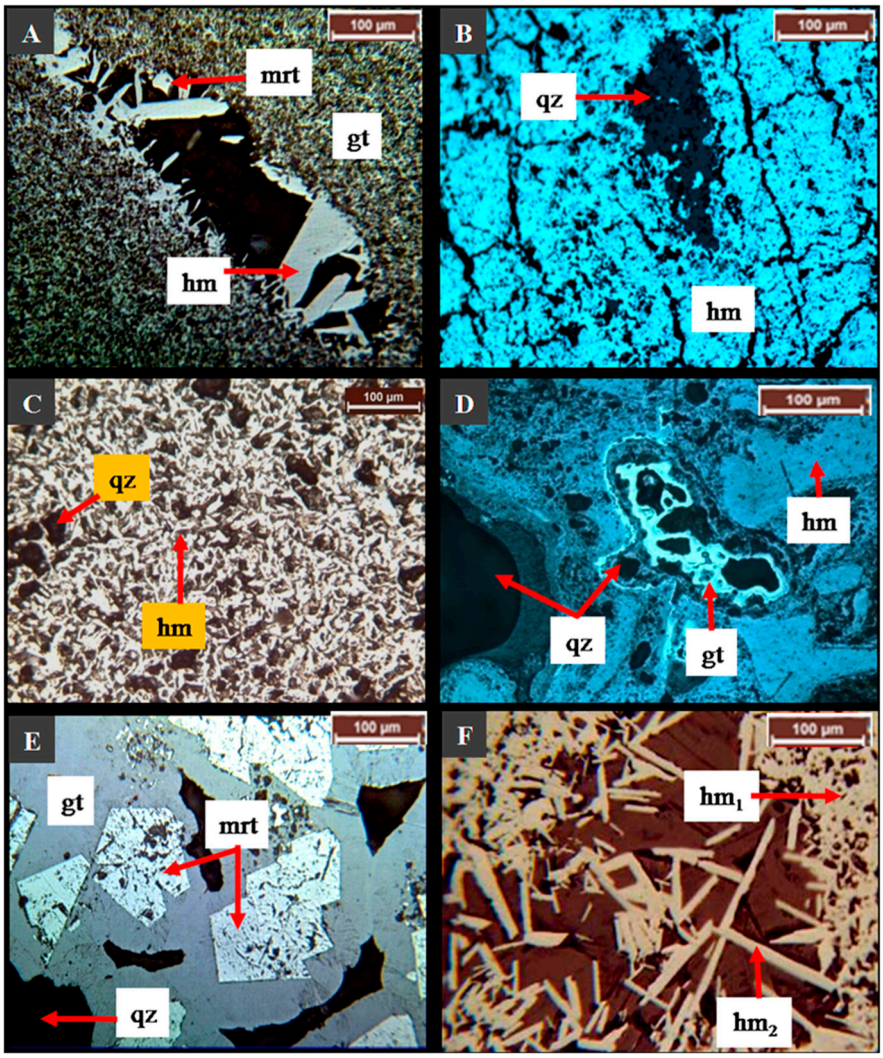

Figure 10. Photomicrographs showing: (**A**) hard massive ore consisting mainly of hematite (hm), martite (mrt) and goethite (gt) along with relict magnetite; (**B**) hard laminated ore consisting of micro-platy hematite (hm) along with quartz (qz) in voids; (**C**) blue dust containing micro-platy hematite (hm) along with fine grained quartz (qz); (**D**) lateritic-goethitic ore showing colloform banding and spheroidal texture, respectively; (**E**) martitized magnetite grains (mrt) in goethitic ore; and (**F**) growth of secondary micro-platy hematite (hm_2) around primary hematite grains (hm_1).

7.3. Soft Laminated Ore

These ores are laminated, highly porous and brittle. Their mineralogy is analogous to the HLO consisting of micro-platy hematite and goethite embedded with smaller grains of quartz (Figure 10B). The textural features of soft laminated ores are almost similar to that of HLO, but there are many voids between the lamellae, and these voids are sometimes filled with secondary minerals such as goethite, gibbsite and clay (kaolinite). They constitute about 60% of total ore types occurring at KMIOD.

7.4. Blue Dust or Friable Powdery Ore

Blue dust is mainly a fine powdery variety of iron ore which has a steel grey color, mainly consisting of micro-platy hematite and martite with a minor amounts of fine grained quartz (Figure 10C). The presence of martite in blue dust indicates its origin through de-silicification of banded varieties of iron ores. The blue dust mainly occurs as pockets and patches depending upon the degree of leaching processes, paleo-channels, lithological and structural attributes. Sometimes,

blue dust is developed along major fractures or joints, which formed due to leaching under supergene enrichment process.

7.5. Goethitic Ore

This type of ore is highly porous in nature. Goethite occurs as colloform bands [31] which are developed due to leaching (Figure 10D). Ore microscopic study shows that these ores are mainly consist of goethite with fine grained hematite (Figure 10D). Hematite occurs as euhedral to subhedral grains surrounded by siliceous matrix. Secondary quartz with clay (kaolinite) is also seen at places in the cavities (Figure 10D,E).

The banded iron-formations of the KMIOD mainly represent oxide facies iron-formation. Mineralogically the different types of iron ores predominantly contain martitized magnetite, and hematite (Figure 10E). XRD peaks (Figure 11A–D) of different iron ore types suggest a dominated hematite occurrence, whereas quartz, kaolinite and gibbsite are the major gangue constituents. Major element geochemistry (Table 2) of different iron ore types of KMIOD indicates higher concentration of Fe_2O_3 in hard laminated ore, soft laminated ore and blue dust. Re-crystallization of cryptocrystalline oxide and silicate phases into equant larger grains are common. Large martitized magnetite grains with sharp grain contacts, defining thin iron-rich layers in the banded iron-formations, are common at KMIOD. The enlargement of mineral grains and growth of secondary micro-platy hematite grains (elongated in nature) around pre-existing large martitized magnetite or hematite grains are common in the Kiriburu-Meghahatuburu iron formations (Figure 10F).

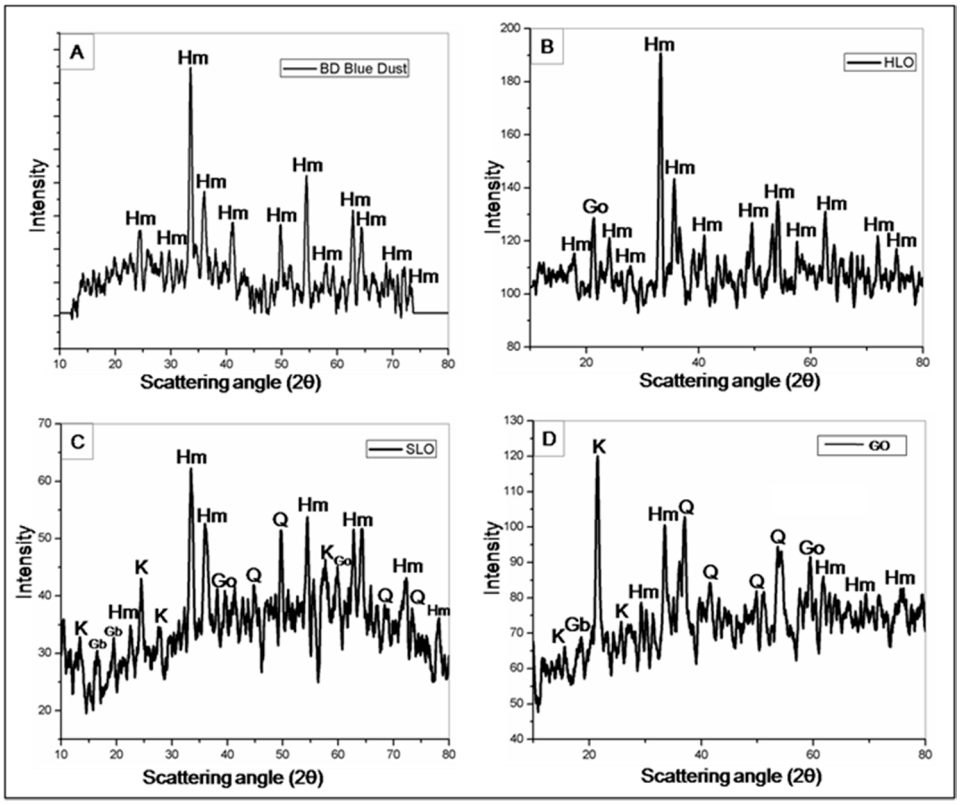

Figure 11. XRD patterns of iron ore samples from Kiriburu-Meghahatuburu iron ore deposit shows the presence of quartz (Q), kaolinite (K), gibbsite (Gb), hematite (Hm) and goethite (Go) in: (**A**) blue dust (BD 1); (**B**) hard laminated ore (HLO 1); (**C**) soft laminated ore (SLO2); and (**D**) goethitic ore (GO1).

Table 2. Major Elemental variation of Kiriburu-Meghahatuburu BHJ and Associated iron ores in wt % (LAT: lateritic-limonitic ore; GO: goethitic ore; HLO: hard laminated ore; SLO: soft laminated ore; BD: blue dust).

Samples wt %	Fe_2O_3	SiO_2	Al_2O_3	P_2O_5	MnO_2	MgO	CaO	TiO_2	S	Na_2O	K_2O	LOI	Total
BHJ1	49.30	45.13	1.50	0.14	0.71	0.06	0.09	0.08	0.04	0.15	0.13	2.30	99.63
BHJ2	50.80	42.23	1.60	0.09	0.63	0.05	0.17	0.21	0.04	0.15	0.06	3.80	99.83
LAT1	72.06	8.37	12.39	0.05	0.17	0.08	0.16	0.17	0.13	0.32	0.03	6.01	99.94
LAT2	73.11	7.42	9.32	0.03	0.22	0.06	0.13	0.12	0.05	0.62	0.11	8.80	99.99
GO1	84.03	5.54	6.65	0.11	0.08	0.10	0.06	0.08	0.04	0.06	0.14	3.11	100.00
GO2	87.72	4.36	3.50	0.11	0.09	0.06	0.05	0.06	0.04	0.05	0.20	3.77	100.01
HLO1	95.00	1.53	1.33	0.05	0.06	0.05	0.04	0.08	0.04	0.04	0.19	1.50	99.91
HLO2	93.80	2.11	2.03	0.08	0.08	0.05	0.05	0.09	0.04	0.05	0.06	1.50	99.94
SLO1	90.80	3.11	2.01	0.10	0.08	0.05	0.05	0.09	0.05	0.05	0.06	3.60	100.05
SLO2	86.92	4.28	2.18	0.07	0.06	0.05	0.06	0.07	0.04	0.05	0.06	6.11	99.95
BD1	95.86	1.75	0.55	0.02	0.20	0.05	0.04	0.08	0.04	0.05	0.05	1.32	100.01
BD2	95.13	2.42	0.91	0.02	0.20	0.05	0.04	0.06	0.04	0.06	0.05	1.02	100.00

8. Geological Controls on Iron Ore Mineralization

The localization and formation of various types of iron ores, their thickness and grade variations impart a combination of lithological, paleoclimatic and structural controls which can be discussed in the following sections.

8.1. Lithological and Paleoclimatic Controls

The iron ores at KMIOD are closely associated with shale and quartzite where porosity, permeability and brittleness of the host rocks could play some role in iron enrichment processes, since they provide channel ways for downward circulation of meteoric solution for leaching and forming different types of iron ores (Figures 3, 6E and 13). The close association of high-grade iron ores, such as blue dust and soft friable ores with BHJ at different mine benches indicate that the genesis of such ores has resulted from BHJ due to supergene ore enrichment processes with gradual removal of silica and alumina (Figure 12A,B). The leaching is a natural process causing removal of soluble substances downward through solution and leaching of gangue constituents (Si, Al) from the inter-bedded ferruginous shale within BIFs, contributing significantly to the formation of powdery ores and pockets of blue dust (Figure 12C).

Iron ore sequences of the area are associated with mafic volcanism at places and are congenial to ore deposition, contributing Fe source to the depositional basin (9) (Figures 4D and 6F). The evolution of thick sequences of hematite deposits is considered to be secondary in nature [6,8,32,33] and originated as a result of supergene enrichment processes (Figures 12 and 13). The iron ore deposits of the area are well marked by the past climatic changes and erosional cycle, which is evidenced by ferruginous-siliceous lateritic ore occupying high elevation zones with large scale silicification and box-work structures associated with the BIFs (Figures 5B and 12B). Weathering of lateritic ores occurring at the top of the deposits resulted in the formation of hard, goethite-rich duricrust above the ore bodies, which protected the underlying high-grade ores from erosion.

Thus, the processes of deep weathering and continuous leaching might have played a vital role for the genesis of high-grade iron ores in the area through removal of silica and alumina under suitable Eh and pH conditions, suggesting paleoclimatic controls on iron formation. The deposition of BIFs in the Singhbhum-Orissa region, took place under increased Eh of depositional fluid and predominance of oxidation [34]. Silica is preferentially leached if the solution is alkaline, whereas alumina and iron are leached under acidic conditions suggesting paleoclimatic control on iron formation [9]. Fe_2O_3/Al_2O_3 ratio may also reflect the composition of protolith.

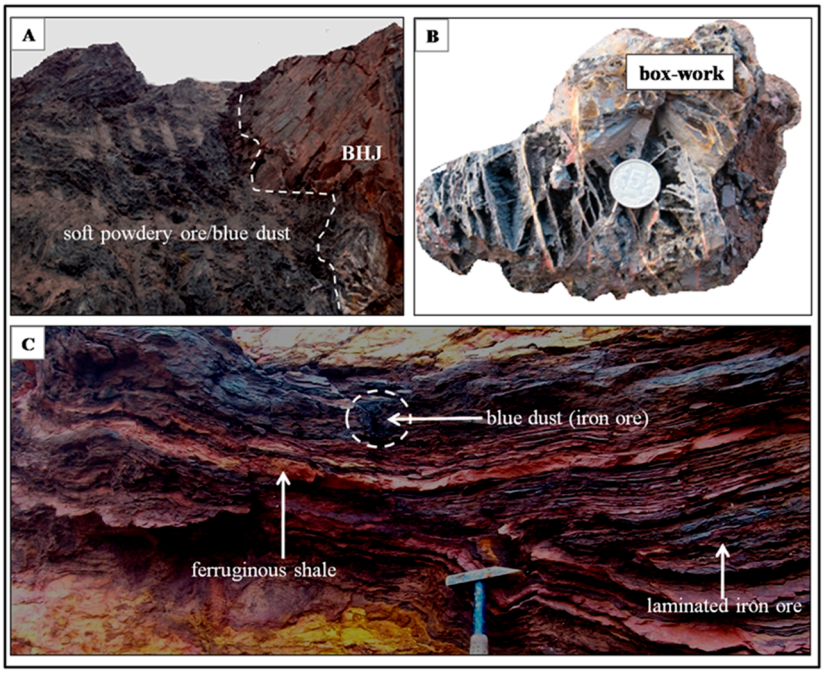

Figure 12. (**A**) Field photograph showing formation of high-grade iron ores (blue dust) from BHJ through leaching processes; (**B**) box-work structure developed in goethitic ore formed due to erosional cycle, indicating paleoclimatic controls on the genesis of high-grade iron ores at KMIOD; and (**C**) inter-bedded ferruginous shale associated with BIFs which leads to the formation of blue dust through continuous leaching processes.

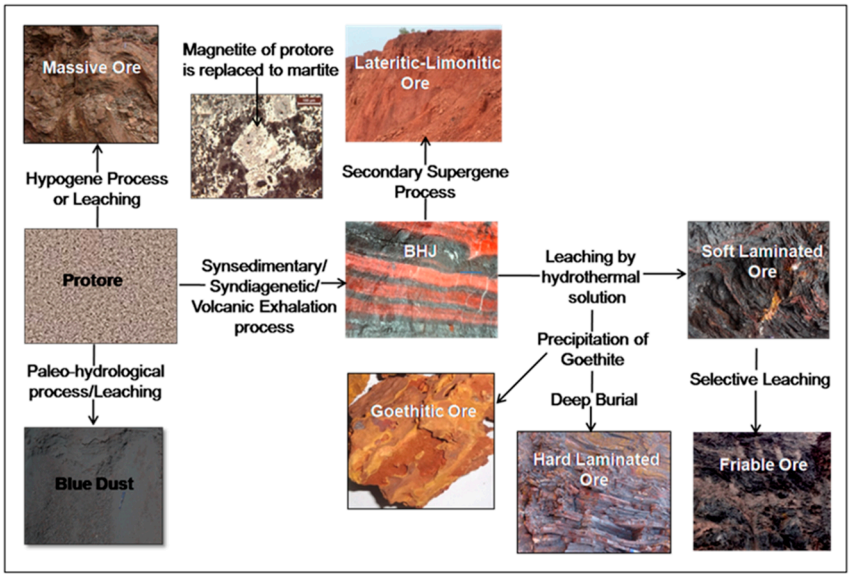

Figure 13. Schematic diagram showing possible evolution of different types of iron ores at KMIOD from proto-ore and BHJ aided by the rheological features of various lithological units modified after [9,34].

Supergene-Modified Hydrothermal Model

This model explains two major stages of iron ore formations [32], i.e., an early hypogene hydrothermal stage where hard micro-platy hematite and martite-rich ore is formed and a late supergene stage where soft, porous hematite and hard, goethite-rich ore is formed (Figure 13). The hydrothermal stage comprises, leaching of silica, formation of magnetite, formation of micro-platy hematite and martite through

martitization by circulation of hydrothermal fluids. Later, during supergene enrichment processes, dissolution of silica takes place while Fe^{2+} goes into solution, thus leading to increase in porosity resulting blue dust formation and re-precipitation of goethite forming flaky ores and hard goethitic or lateritic ores (Figure 13).

Nevertheless, it is observed that despite having some common features, the BIFs are not likely to fit into a single depositional model due to lack of uniform genetic model during a long depositional event, different geological conditions and difference in depositional settings. Hence, magnetite-martite mineralogy, presence of oxidized BHJ, micro-platy hematite, soft laminated ores, blue dust, goethitic and lateritic ores along with lithological and structural attributes are some of the evidences thatsupport a hydrothermal model as well as a supergene process for the genesis of iron ores at KMIOD from the primarily deposited BHJ (Figures 10–14). Based on these evidences, a "supergene-modified hydrothermal model" may be proposed as a possible model for the evolution of iron ore deposits of Kiriburu-Meghahatuburu area.

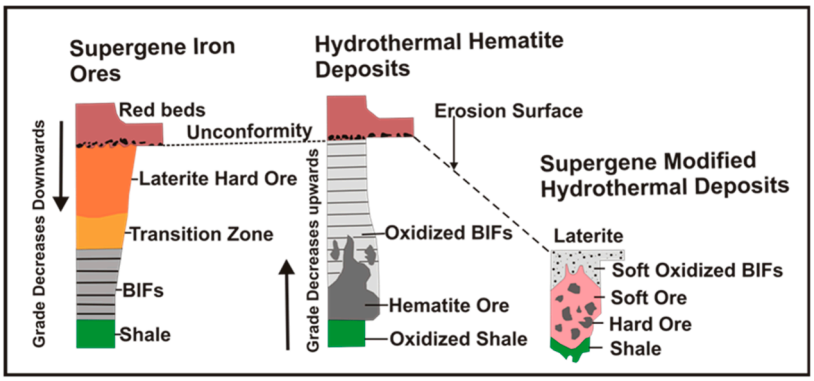

Figure 14. Schematic diagram showing supergene-modified hydrothermal process for the formation of different types of iron ores at Kiriburu-Meghahatuburu region from the BIFs modified after [32].

8.2. Structural Controls

Structural information of BIFs is greatly emphasized to formulate the exploration plan which leads to the discovery of deposits or extension of iron ore bodies in existing deposit. Structural set up of the depositional environment results in formation of iron ores with distinct micro-structural and textural features and variable physical properties. The structural features determine the location of the ore bodies in two ways, i.e., forming a pathway allowing access for supergene or hypogene fluids from a suitable source to the site of ore formation and secondly, providing a mechanism for the preservation of mineralized systems by protecting the newly formed ore bodies from erosion.

KMIOD lies within one of the structurally and tectonically complex active zones in the eastern Indian geological history. Structural elements including various types of folds, fault arrays and joints acted as loci for high-grade iron ore deposition in the area. The iron ore deposits are seen striking towards a NE–SW direction with an average dip amount of 65°, varying from 55° to 85°, dipping towards a W–NW direction (Figures 8 and 9). Hence, the steepness of beds with higher elevation (up to 88°) has enhanced the leaching processes and subsequent enrichment of iron, forming high-grade iron ores such as blue dust or soft friable ores, as noted in the open cast mining area (Figure 12A). The extensive field studies combined with exhaustive exploration data, especially from the mine sites, have shown that the concentration of most of the high-grade iron ore bodies are located along the hinge portion of the second generation (F_2) folds, which are tight in nature with a fold axis trending NE–SW due to easy access for circulation of meteoric solutions along the fractures developed due to release of stresses (Figure 8A).

Thus, understanding the differential geometry of BIFs and iron ore bodies that are principally along hinge portions of large-scale fold structures is crucial to decipher the future exploration and

reserve calculations of iron ore resources within the iron ore belt [35]. Hence, the various structural elements including second generation tight folds, faults, closely spaced joint network and fracture arrays seems to be provided conduits for downward migration of fluids for the supergene ore enrichment processes. These processes have caused removal of deleterious elements such as silica and alumina from the system and formation of high-grade iron ores in the area. The BIFs must have been exposed to the surface to facilitate leaching of iron in the vadose zone and groundwater would have percolated downward along pre-existing fractures and fault arrays [36,37]. The gangue minerals such as silica and alumina would have leached with these fluids and replaced them with secondary goethite, resulting in soft friable ore or high-grade blue dust ore. Spatial occurrence of different iron ore grades within the open cast mine and correlation along sub-surface boreholes at different elevations (Figure 15A,B) in the study area are indicators of effective leaching and enrichment process that lead to the formation of high-grade iron ores.

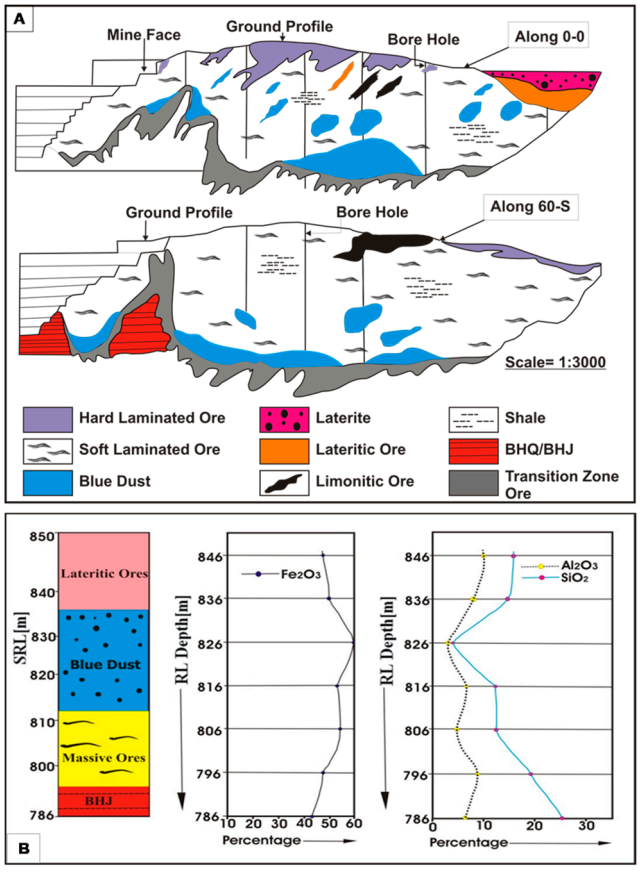

Figure 15. (**A**) Geological cross section along bore holes at KMIOD showing variable grades of iron ores imparting strong controls of various structural elements for the genesis of the iron ores; and (**B**) detailed drill-hole core log of iron ore deposit showing variation of Fe_2O_3, $SiO_2$and Al_2O_3at depth and their variability between different types of iron ores.

The bulk geochemical data of KMIOD (Table 2) confirms that the high-grade ores such as blue dust are strongly enriched in iron and depleted in SiO_2, Al_2O_3, MgO, CaO and other major elements and are analogous to the high-grade ores such blue dust ore of the other world BIFs such Ruth Lake Areas, Western Labrador (Fe_2O_3: 93.90 wt %; SiO_2: 3.0 wt %; Al_2O_3: 0.4 wt %; MgO: 0.03 wt %; CaO: 0.03 wt %, Na_2O: 0.05 wt %; K_2O: 0.05 wt %; TiO_2: 0.04 wt % and P_2O_5: 0.07 wt %) [37]. Hence, the high-grade ores strongly enriched in Fe and depleted in SiO_2, CaO and MgO, indicates leaching of SiO_2 during supergene ore enrichment processes of the ore formation aided by various structural features.

9. Conclusions

The iron ore sequence of Kiriburu-Meghahatuburu (>150 MT) occurs as a supracrustal suite along the BKIOB or Noamundi Basin and is closely associated with BHJ, quartzite, tuffaceous and ferruginous shale, mafic volcanic rock and autoclastic conglomerate. These deposits are mainly located towards the western limb of the horseshoe-shaped synclinorium within BKIOB. The BHJ and associated high-grade iron ores (62.85 $\pm$ 1.31 wt % Fe) experienced three phases of successive deformations (D_1, D_2 and D_3) with numerous structures such as banding, bedding, folds, minor faults and joints (26 and 25). The field studies corroborated with lithological, structural and borehole data interpretation and petrographic studies of the host rocks and associated iron ores show a combination of lithological, paleoclimatic and structural controls on the localization and genesis of the high-grade iron ores such as blue dust (~67% Fe) at KMIOD.

Lithologically, the BIFs are governed by rheological features providing channel ways in the ore enrichment process. The BHJ and interbedded ferruginous shale seems to have been given a significant contribution for the formation of different grades of iron ores over the area (Figure 12A–C). The area could have represented arid-tropical climates, high altitudes with high rainfall, erosional cycles and subsequent paleoclimatic changes helped in the formation of blue dust and powdery ores which can be evidenced by the presence of thick lateritic capping, silicification and box-work structures indicating paleoclimatic controls on the genesis of the iron ores (Figure 12C).

Structurally, the BHJ-hosted iron ores are principally controlled by the structural features such as folds, fault arrays, joint network and fractures, which might have controlled the migration of ore fluids aided with supergene ore enrichment processes. The steeply dipping (even up to 75°–88°) bedding planes might have enhanced the leaching processes and enriched the BIFs forming high-grade iron ores in the area. Field studies along with subsurface data depict that the deposits are mainly associated with the second generation (F_2) folds with NE–SW trends and concentration of most of the high-grade iron ore bodies are located along the hinge portion of these folds. Hence, understanding the structural geometry along with lithological variation of BIFs and iron ore bodies within hinge portions of large-scale fold structures is crucial for planning future exploration program and grade recovery of iron ore resources at KMIOD and in the adjoining analogous areas.

Acknowledgments: The authors thank General Manger (Mines) of M/s Steel Authority of India Limited (SAIL), Meghahatuburu Iron Ore Mine, Raw Materials Division for providing necessary permissions and facilities. Thanks are also due to Director, Indian Institute of Technology (Indian School of Mines), Dhanbad, India for providing necessary facilities. The authors thank Department of Science and Technology, Government of India for the support through DST-FIST Level II grants to Applied Geology Department, IIT(ISM) Dhanbad. We extend our gratitude to the editorial team for their cooperation and assistance during the manuscript handling. We would like to thank the Editor-in-Chief, academic editor and two anonymous reviewers for their extensive review, valuable comments and suggestions for improving the quality of the manuscript.

Author Contributions: J.P. conducted field studies, collected data sets and prepared the draft paper as part of his Ph.D. research work. A.S.V. supervised and interpreted the data. P.R.S. analyzed and interpreted chemical data. S.S. and N.S.K. participated in technical discussions.

Conflicts of Interest: The authors declare no conflict of interest.

References

1. Jones, H.C. The iron ore deposits of Bihar and Orissa. *Mem. Geol. Surv. India* **1934**, *63*, 167–302.
2. Spencer, E.; Percival, F.G. The Structure and origin of Banded Hematite Jaspers of Singhbhum, India. *Econ. Geol.* **1952**, *67*, 365–385. [CrossRef]
3. Rai, K.L.; Sarkar, S.N.; Paul, P.R. Primary depositional and diagenetic features in Banded Iron Formation and associated iron ore deposits of Noamundi, India. *Mineral. Depos.* **1980**, *15*, 189–200. [CrossRef]
4. Saha, A.K. Crustal evolution of Singhbhum-North Orissa, eastern India. *Mem. Geol. Soc. India* **1994**, *27*, 1–341.
5. Ghosh, G.; Mukhopadhyay, J. Reappraisal of the structure of the Western Iron Ore Group, Singhbhumcraton, eastern India: Implications for the exploration of BIF-hosted iron ore deposits. *Gond. Res.* **2007**, *12*, 525–532. [CrossRef]

6. Mukhopadhyay, J.; Gutzmer, J.; Beukes, N.J.; Bhattacharya, H.N. Geology and Genesis of the Major Banded Iron Formation-Hosted High-Grade Iron Ore Deposits of India. *Rev. Econ. Geol.* **2008**, *15*, 291–316.
7. Beukes, N.J.; Mukhopadhyay, J.; Gutzmer, J. Genesis of high grade iron ores of the Archean Iron Ore Group around Noamundi, India. *Econ. Geol.* **2008**, *103*, 365–368. [CrossRef]
8. Majumder, T.; Chakraborty, K.L.; Bhattacharjee, A. Geochemistry of Banded Iron-Formation of Orissa. *India. Mineral. Depos.* **1982**, *17*, 107–118. [CrossRef]
9. Roy, S.; Venkatesh, A.S. Mineralogy and geochemistry of banded iron formation and iron ores from eastern India with implications on their genesis. *J. Earth Syst. Sci.* **2009**, *118*, 1–23. [CrossRef]
10. Majumder, T.; Chakraborty, K.L. Petrography and petrology of the Precambrian Banded Iron Formation of Orissa, India and reformation of the bands. *Sed. Geol.* **1979**, *22*, 243–265. [CrossRef]
11. Bhattacharya, H.N.; Chakraborty, I.; Ghosh, K.K. Geochemistry of some Banded Iron Formations of the Archaean supracrustals, Jharkhand-Odisha region, India. *J. Earth Syst. Sci.* **2007**, *116*, 245–259. [CrossRef]
12. Chakraborty, K.L.; Majumder, T. Geological Aspects of the Banded Iron Formation of Bihar and Orissa. *J. Geol. Soc. India* **1986**, *28*, 109–133.
13. Roy, S.; Venkatesh, A.S. Banded Iron Formation to Blue Dust: Mineralogical and Geochemical constraints from the Precambrian Jilling-Langalata Deposits, Eastern Indian Craton. *Appl. Earth Sci. (Trans. Inst. Min. Metall. B)* **2009**, *118*, 178–188. [CrossRef]
14. Upadhyay, R.K.; Venkatesh, A.S.; Roy, S. Iron ore deposits of eastern India: Geological aspects and their mineralogical Characteristics. *Resour. Geol.* **2010**, *60*, 203–211. [CrossRef]
15. Klein, C.; Beukes, N.J. Geochemistry and sedimentology of a facies transition from limestone to iron formation deposition in the Early Proterozoic Transvaal Supergroup. *S. Afr. Econ. Geol.* **1989**, *84*, 1733–1774. [CrossRef]
16. Trendall, A.F. The significance of iron formation in the Precambrian stratigraphic record. In *Precambrian Sedimentary Environments: A Modern Approach to Ancient Depositional Systems*; Altermann, W., Corcoran, P.L., Eds.; Blackwell Publishing Ltd.: Oxford, UK, 2002.
17. Ilouga, D.C.I.; Suh, C.E.; Tanwi, G.R. Textures and Rare Earth Elements Composition of Banded Iron Formations (BIF) at Njweng Prospect, Mbalam Iron Ore District, Southern Cameroon. *Int. J. Geosci.* **2013**, *4*, 146–165. [CrossRef]
18. Lascelles, D.F.; Tsiokos, D.S. Microplaty hematite ore in the Yilgarn Province of Western Australia: The geology and genesis of the Wiluna West iron ore deposits. *Ore Geol. Rev.* **2015**, *66*, 309–333. [CrossRef]
19. Bekker, A.; Planavsky, N.J.; Krapez, B.; Rasmussen, B.; Hofmann, A.; Slack, J.F.; Rouxel, O.J.; Konhauser, K.O. Iron Formations: Their Origins and Implications for Ancient Seawater Chemistry. *Treatise Geochem.* **2014**, *9*, 561–628.
20. Dunn, J.A. The mineral deposits of eastern Singhbhum and surrounding areas. *Mem. Geom. Surv. India* **1937**, *69*, 197–206.
21. Dunn, J.A.; Dey, A.K. Geology and petrology of eastern Singhbhum and surrounding areas. *India. Geol. Surv. Mem.* **1942**, *69*, 281–456.
22. Sarkar, S.N.; Saha, A.K. The present status of Precambrian stratigraphy, tectonics and geochronology of Singhbhum-Keonjhar-Mayurbhanj region India. *Ind. J. Earth Sci.* **1977**, *S Ray Volume*, 37–65.
23. Saha, A.K.; Ray, S.I.; Sarkar, S.N. Early history of the Earth: Evidence from the eastern Indian shield. *Geol. Soc. India Mem.* **1988**, *8*, 13–37.
24. Mamtani, M.; Mukherjee, A.; Chaudhuri, A.K. Microstructures in a banded iron formation (Gua mines, India). *Geol. Mag.* **2007**, *144*, 271–287. [CrossRef]
25. Sosnicka, M.; Bakker, R.J.; Broman, C.; Pitcairn, I.; Paranko, I.; Burlinson, K. Fluid types and their genetic meaning for the BIF-hosted iron ores, Krivoy Rog, Ukraine. *Ore Geol. Rev.* **2015**, *68*, 171–194. [CrossRef]
26. Li, W.; Beard, B.L.; Johnson, C.M. Biologically recycled continental iron is a major component in banded iron formations. *Proc. Natl. Acad. Sci. USA* **2015**, *112*. [CrossRef] [PubMed]
27. Hagemann, S.G.; Angerer, T.; Duuring, P.; Rosière, C.A.; Figueiredo e Silva, R.C.; Lobato, L.; Hensler, A.S.; Walde, D.H.G. BIFs-hosted iron mineral system: A review. *Ore Geol. Rev.* **2016**, *76*, 317–359. [CrossRef]
28. Mukherjee, A.; Chaudhuri, A.K.; Mamtani, M.A. Regional scale strain variations in Banded Iron Formations of Eastern India: Results from anisotropy of Magnetic susceptibility studies. *J. Struct. Geol.* **2004**, *26*, 2175–2189. [CrossRef]

29. Gross, G.A. A classification of iron-formation based on depositional environments. *Can. Min.* **1980**, *18*, 215–222.
30. Ramsay, J.G.; Huber, M.I. The Techniques of Modern Structural Geology. In *Folds and Fractures*; Academic Press: London, UK, 1987; Volume 2, pp. 309–700.
31. Ramdohr, P. *The Ore Minerals and Their Intergrowths*; Pergamon Press: Oxford, UK, 1980; Volumes 1–2, p. 1207.
32. Beukes, N.J.; Gutzmer, J.; Mukhopadhyay, J. The geology and genesis of high grade hematite iron ore deposits. *Appl. Earth Sci. (Trans. Inst. Min. Metall. B)* **2003**, *112*, 18–24. [CrossRef]
33. Upadhyay, R.K.; Asokan, S.; Venkatesh, A.S. Mode of occurrence of phosphorous in iron ores of eastern limb, Bonai synclinorium, eastern India. *J. Geol. Soc. India* **2011**, *77*, 549–556. [CrossRef]
34. Mukhopadhyay, A.; Chanda, S.K. Silica diagenesis in the banded hematite jasper and bedded chert associated with the Iron Ore Group of Jamda-Koira valley, Orissa, India. *Sed. Geol.* **1972**, *8*, 113–135. [CrossRef]
35. Prasad, J.; Venkatesh, A.S.; Chaturvedi, L. Geological Aspects of Iron Ores from Kiriburu-Meghahatuburu: Implications for Exploration, Value Addition and Mining Operation. In Proceedings of the 6th National Seminar on Surface Mining, New Delhi, India, 10–11 January 2014; pp. 467–474.
36. Morris, R.C.; Kneeshaw, M. Genesis modelling for the Hamersley BIF-hosted iron ores of Western Australia: A critical review. *Aust. J. Earth Sci.* **2011**, *58*, 417–451. [CrossRef]
37. Conliffe, J. Geology and geochemistry of high-grade iron-ore deposits in the Kiviviv, Timmins and Ruth Lake areas, Western Labrador. *Curr. Res.* **2016**, *16*, 1–26.